Titanate nanotubes and nanosheets as a mechanical reinforcement of water-soluble polyamic acid: Experimental and theoretical studies

Christian Harito[1], Dmitry V. Bavykin[1], Mark E. Light[2], Frank C Walsh[1]

1. Energy Technology Research Group, Faculty of Engineering and the Environment, University of Southampton, SO17 1BJ, Southampton, U.K.

2. School of Chemistry, Faculty of Natural and Environmental Sciences, University of Southampton, SO17 1BJ, Southampton, U.K.

Abstract. Titanate nanosheets (TiNS), titanate nanotubes (TiNT), and scrolled titanate nanosheets (STiNS) were used to synthesise polymer nanocomposites by solution processing. The hardness was found to increase by 90% on addition of 2% TiNS while the modulus (*Er*) increased by 103% compared to the pure polymer. Small angle X-ray scattering (SAXS) measurements of composite films were used to study alignment of nanostructures within the polymer. The obtained data on mechanical properties of composites have been tested against theoretical values and it was established that both nanostructures alignment as well as their mechanical properties affect the hardness and modulus of the polymer composites. At a low content of TiNS, the reinforcement behaviour matched well with Halpin-Tsai theory which assumes the filler has unidirectional orientation. After addition of 2 wt% TiNT, the hardness and modulus of the polyamic acid salt composites increased by 91% and 165%, respectively, and were higher than theoretical predictions, indicating that both TiNT and STiNS, prepared by hydrothermal synthesis, may have higher mechanical properties than bulk TiO_2. At a high filler loading (>2 wt%), the mechanical properties of composites do not fit established theories due to agglomeration of titanate nanostructures.

Key words: A. Nanostructures, A. Polymer-matrix composites (PMCs), B. Mechanical properties, C. Micro-mechanics

1. Introduction

Polymer nanocomposite materials consist of a hybrid organic matrix containing dispersed nanostructure filler. The structures are widely varied from zero (sphere, cubes, and polyhedrons), one (rods, fibres, tubes), two (sheets, discs, plates) dimensional, and complex shapes (flower, leaf, etc.) These nanofillers provide significant improvement in the polymer properties at low filler loadings due to the large degree of contact between nanofiller and polymer. For example, the small addition of exfoliated clay (4.7 wt%) can increase the flexural modulus of nylon-6 by four times at 120 ^{o}C [1]. Successful application of clay filler to improve the mechanical properties of polymers requires further research on other nanostructure based polymer nanocomposites containing, e.g., metal oxides, hydroxides, nitrides, and chalcogenides. In the past decades, titanium oxide with various structures (e.g., nanotubes and nanosheets) has been studied. Titanium oxide single layer nanosheets (TiNS), the graphene analogue, have been discovered by Sasaki, *et.al.* [2] in the mid-1990s. These nanosheets can be obtained by a three-step process involving solid-state reaction, acid ion-exchange, and exfoliation [2]. The resulting product is a highly crystalline single layer sheet possessing unique properties which differ from bulk titanium oxide [3]. These nanosheets have been applied in various functional nanocomposite polymers, for example acting as photo-initiators for water-soluble vinyl monomers polymerisation owing to the photocatalytic properties of titanate nanosheets [4]. Proton-donating monomers such as N-isopropylacrylamide (IPAAm), acrylamide (AAm), and acrylic acid (AAc) may produce strong bonds to the negatively charged titanate nanosheets and polymerize with TiNS as a physical photo-crosslinker. The polymerization occurs near the TiNS and the polymer is trapped by adjacent TiNS producing a highly sensitive optical response to thermal stimuli. The proton conductivity of sulfonated poly(ether ether ketone) (SPEEK) membranes is enhanced by up to two times by low loading of titanate nanosheets (1.67 wt%) [5]. Such

materials are stable at high temperatures (140 ^{o}C) and in a wet environment (100 % relative humidity). Adding TiNS to polyethylene naphthalate (PEN) films significantly decreases helium gas permeability [6]. However, there is no systematic study on the mechanical reinforcement effects of titanate nanosheets on polymer nanocomposite.

In contrast to titanate nanosheets, titanate nanotubes (TiNT) only require a one-step alkaline hydrothermal treatment. Alkali treatment at high temperature (*ca.* 110 ^{o}C) induces scrolling of the titanate nanosheets producing titanate nanotubes [7]. This kind of nanotubes was discovered in 1997 by Kasuga, *et.al.* [8]. Incorporation of elongated titanates into the polymers can improve the transport properties in nanofiltration membranes [9], gas sorption capacity [10], corrosion resistance [11], and thermal properties [12]. It has also been used to strengthen polymer blends such as polyethylene oxide and chitosan [13]. At 25 wt% loading of titanate nanotubes, the polymer blend was found to be approximately 2.6 times harder compared to the neat polymer blend and 3.4 times stiffer. Considering this promising enhancement of nanofiller at low loadings, the reinforcement effect needs to be further studied. Instead of nanotubes, the alkaline hydrothermal method can also produce nanosheets with scrolled morphology at lower processing temperatures [7]. The study of these scrolled nanosheets (STiNS) is still very limited. Titanate nanotubes and scrolled nanosheets due to the simplicity of their manufacturing and abundance of the precursors, can be useful low cost alternative to carbon nanostructures such as graphene and carbon nanotubes for certain applications (e.g., structural, thermal protection, gas and UV barrier).

In this work, titanate nanotubes (TiNT), scrolled titanate nanosheets (STiNS), and titanate nanosheets (TiNS) have been used to enhance the mechanical properties of water soluble polyimide precursors, namely, polyamic acid salt (PAAS). Titanate nanotubes and nanosheets possess high surface charges making them easily dispersed and stabilised in aqueous solvent, hence the choice of water-soluble polymers. Moreover, the polyamic acid

salt is a more stable form of polyamic acid which is the polyimide precursor [14]. The morphology of the titanate nanosheets and nanotubes were examined with scanning electron microscopy (SEM) and transmission electron microscopy (TEM). Nanoindentation has been used to study the reduced modulus (*Er*) and hardness (*H*) of the composites. Experimental results are compared with theoretical models, such as those due to the modified rule of mixtures [15], Halpin-Tsai [16], and Halpin-Kardos [17], to study and evaluate the existing models. The dispersion of titanate nanosheets and nanotubes in polyamic acid is studied by TEM to determine its correlation with mechanical properties and compared to that of the titanate nanostructures-polyamic acid salt composite. Small-angle x-ray scattering (SAXS) was used to determine the interlayer spacing of nanosheets inside the polymer, to confirm incorporation of nanotubes within the polymer and investigate the degree and alignment of nanostructures.

2. Theoretical background and experimental

It is important to study the experimental data alongside existing theoretical models. Clay [18], graphene [19], and carbon nanotubes [20] are often used to evaluate micromechanical models for nanocomposite reinforcement. Herein, we report titanate nanotubes, scrolled titanate nanosheets, and titanate nanosheets as a mechanical reinforcement of water-soluble polyamic acid.

2.1. Theoretical background

The theoretical models used in this particular research are models able to predict composites containing matrix and filler as reinforcements with the basic assumptions of a

void free matrix and no residual stress in composites (stress-free state). Modified rule of mixtures, Halpin-Tsai, and Halpin-Kardos were chosen for this purpose.

2.1.1. Modified rule of mixtures

The rule of mixtures is a well-known model based on the Voigt equation [21] that is used to predict continuous unidirectional fibre composites. This model is also known as the iso-strain model which assumes the filler and matrix have the same elongation when a certain load is applied to the composite. However, it is not suitable for evaluating mechanical properties of some composites as it often overestimates the properties [22,23]. Hence, the modified rule of mixtures, which is a semi-empirical model, is applied [15]. The modified rule of mixtures is:

$$E_c = \chi_f E_f V_f + E_m(1 - V_m) \quad (1)$$

where E_c, E_f, and E_m are the moduli of composite, filler, and matrix, respectively. χ_f is a particle strengthening factor with values between 0 and 1. V_f and V_m are the volume fractions of filler and matrix obtained by converting the weight filler fractions, assuming the densities of TiO_2 (4.23 g ml^{-1}) and polyamic acid (1.04 g ml^{-1}). This equation can also be applied to estimate the hardness of the composite by substituting the modulus for hardness. The modulus and hardness of the filler is taken from CRC Materials Science and Engineering Handbook [24], which are 282.76 GPa and 10.99 GPa, respectively, considering TiNS, STiNS, and TiNT structures as TiO_2. The Young's modulus and hardness of the matrix are adapted from nanoindentation of the polyamic acid salt

2.1.2. Halpin-Tsai equation

The Halpin-Tsai equation is a model to estimate reinforcement of unidirectional oriented short fibres and has successfully predicted the reinforcement of carbon nanotubes at low filler content (>1 wt%) [25]. It can also be adapted to predict the modulus of polymer nanocomposites with nanosheets (e.g., clay [18] and graphene [26]) as filler. The Halpin-Tsai equation is:

$$\frac{E_c}{E_m} = \frac{1+2A_f\mu\phi_f}{1-\mu\phi_f} \quad (2)$$

where E_c and E_m are the moduli of the composite and matrix (PAAS), respectively. The Young's modulus of the matrix (PAAS) is adapted from nanoindentation measurements of pure PAAS. A_f is the filler aspect ratio (l/h), in this case (l) is the nanosheets or nanotubes length and (h) is the nanosheets thickness or nanotubes diameter. Φ_f is the volume fraction of filler. μ is a geometric factor, given by:

$$\mu = \frac{(E_f/E_m)-1}{(E_f/E_m)+2A_f} \quad (3)$$

where E_f is the modulus of TiO_2 taken from literature [24]. The Halpin-Tsai equation is also able to predict the hardness of micro and nanocomposites by simply exchanging the modulus with hardness [27]. The hardness of the matrix (H_m) is determined by nanoindentation of pure PAAS while the hardness of TiO_2 (10.99 GPa) is taken from the literature [24].

2.1.3. Halpin-Kardos equation

Originally, the Halpin-Kardos equation was applied to randomly oriented short fibres with a quasi-isotropic laminate assumption involving the $[0/+45/90/-45]_n$ configuration [17]. However, the expression can also be adapted. It has been successfully used to predict the reinforcement of nanosheets (e.g., clay) up to 2 wt% in a polymer blend [18]. The authors

argued that the tactoid phase of clay may act in a similar fashion to short fibres. The Halpin-Kardos equation is:

$$\frac{E_c}{E_m} = \frac{3}{8}\left[\frac{1+2A_f\eta_L\phi_f}{1-\eta_L\phi_f}\right] + \frac{5}{8}\left[\frac{1+2\eta_T\phi_f}{1-\eta_T\phi_f}\right] \quad (4)$$

where E_c and E_m are the moduli of the composite and matrix respectively. A_f is the aspect ratio of the filler (l/h) where l is the nanosheets or nanotubes length and h is the nanosheets thickness or nanotubes diameter. Φ_f is the filler volume fraction. η_L and η_T can be determined from the following equations:

$$\eta_L = \frac{(E_f/E_m)-1}{(E_f/E_m)+2A_f} \quad (5)$$

$$\eta_T = \frac{(E_f/E_m)-1}{(E_f/E_m)+2} \quad (6)$$

where E_f is the modulus of TiO_2 [24]. To obtain the hardness, this equation was modified by substituting the modulus for hardness.

2.2. Experimental

2.2.1. Synthesis of Sasaki's titanate nanosheets

A synthesis method for single-layer titanate nanosheets is adapted from Sasaki, *et.al.* [28]. Sasaki's single-layer titanate nanosheets are based on two starting materials that are an alkali precursor (K, Li, Rb, Cs) and a TiO_2 powder. For the synthesis of titanate nanosheets by the Cs route, TiO_2 (Degussa P25) from Aeroxide and Cs_2CO_3 from Sigma-Aldrich were used without further purification.

There are three steps to synthesis single-layer titanate nanosheets. Firstly, the solid-state reaction of TiO_2 and Cs_2CO_3 was conducted based on the work of Grey, *et.al.* [29]. 2.6 g of Cs_2CO_3 and 2 g of TiO_2 (molar ratio 1 : 5.3) were mixed, ground, and put into a platinum crucible (an inert crucible is crucial to prevent reaction of alkali precursor and crucible) for one hour heating at 800 ^oC. The mixture was allowed to cool down to ambient temperatures naturally. Next, it was ground and two cycles of heating at 800 ^oC for 20 h were conducted with grinding between cycles. The resulting product is a white powder of lepidocrocite-like caesium titanate ($Cs_{0.7}Ti_{1.825}\square_{0.175}O_4$) with $\square$ representing a vacancy. The second step includes an acid ion-exchange that was performed to create a smectite-like acid titanate ($H_{0.7}Ti_{1.825}\square_{0.175}O_4 \cdot H_2O$). 2.4 g of $Cs_{0.7}Ti_{1.825}\square_{0.175}O_4$ were stirred with 96 ml of 1 M HCl for 4 days. The acid solution was replaced with a fresh acid solution every day to maintain the concentration of H^+ ions for acid leaching of Cs^+ ions. Next, the solution was decanted with deionized (DI) water three times followed by vacuum filtration using a 0.2 μm nylon membrane and washed with distilled water until the conductivity reached *ca.*10 μS cm^{-1}.

During last step, the bulky molecules of triethylamine (TEA) were allowed to ion-exchange the solid sample accompanied by the exfoliation of single layer nanosheets. 0.08 g of $H_{0.7}Ti_{1.825}\square_{0.175}O_4 \cdot H_2O$ was mixed with 20 ml of distilled water and 400 μl of TEA in an ultrasonic bath for 9 h. The solution was kept for 4 days to separate non-exfoliated sheets at the bottom. The exfoliated nanosheets at the top fraction were directly used to make composites.

2.2.2. Synthesis of titanate nanotubes and scrolled nanosheets by hydrothermal methods

Our previous work [7] has been adapted as a methodology for titanate nanotubes (TiNT) and nanosheets (STiNS) synthesis by hydrothermal methods. 25 g of TiO_2 (Degussa P25, Aeroxide) were refluxed with 10 M of a mixture of KOH:NaOH (1:25) (Sigma-Aldrich) in a PFA (perfluoroalkoxy polymer) round-bottom flask (Bohlender GmbH) for 2 days at 106 ^oC to synthesise TiNT. For STiNS, 20 g of TiO_2 and 10 M NaOH were refluxed for 2 weeks at 60 ^oC. The resulting sodium titanate powders ($Na_2Ti_3O_7$) were filtered by vacuum filtration and washed with distilled water until the washing solution reached pH 7. Next, the protonated titanate ($H_2Ti_3O_7$) was formed by washing sodium titanate with an excess of 0.1 M HCl (Sigma-Aldrich) for more than 30 min at 22 ^oC until a stable pH value of 2 was reached, followed by distilled water washing to pH 5. Finally, 0.08 g of protonated titanate ($H_2Ti_3O_7$) mixed with 20 ml of distilled water and 400 µl TEA was sonicated for 9 h in ultrasonic bath. After 4 days of decanting, the top fraction containing non agglomerated TiNT or STiNS was collected used for preparation of the composites.

2.2.3. Synthesis of the polyamic acid salt

The work of Lee, *et.al.* [30] has been used to synthesise a polyamic acid salt. An aromatic polyamic acid salt was prepared from pyromellitic dianhydride (PMDA) and 4,4'-oxydianiline (ODA) as monomers and N,N-Dimethylacetamide (DMAc) as a solvent. All the reactions were shielded by nitrogen gas. As a typical example, a mixture of 1.201 g of ODA (1 mol) and 22.59 g of DMAc was stirred inside a 250 ml round bottom flask at room temperature. After the ODA dissolved, 1.309 g of PMDA (1 mol) was added to the solution and stirred for 1 day, yielding a 10 wt% DMAc solution of polyamic acid. Then, 1.656 ml of triethylamine (TEA), equivalent to 2 mol of monomer, was added. Local white precipitation was visible upon addition of TEA into the solution as stated from Kreuz, *et.al.* [31] and

disappeared after approximately 30 min. The resulting solution was poured into acetone and filtered with a nylon membrane (0.2 µm pore size) followed by washing with acetone twice. After drying at 22 ^{o}C for 24 hours, a light yellow PAAS powder was collected and stored at 22 ^{o}C and 40±5% relative humidity. For the pure polymer film, 0.215 g of PAAS was stirred in 4 ml distilled water and 80 µl TEA to assist dissolution of PAAS, yielding 5 wt% of PAAS in aqueous solution. The solutions were stirred for 3 days and drop cast on glass. The drop cast solutions were kept at 22±2 ^{o}C and 40±5% relative humidity for 4 days to dry and achieve an equilibrium moisture content in the films.

2.2.4. Synthesis of the polyamic acid salt-titanate nanocomposite

All composites (TiNS-PAAS, TiNT-PAAS and STiNS-PAAS) were prepared by solution mixing. A given volume of colloidal solution of known concentration (determined by UV-vis spectrometry) of titanate nanostructures (e.g., TiNS, STiNS, and TiNT) was mixed with 5 wt% aqueous solution of PAAS. The ratio between two solutions was selected to obtain composites with following loading of nanostructures (0.5, 1, 2, 3, and 5 wt% of solid). The mixed solution was vigorously stirred for 3 days and drop cast on glass substrate. The deposited films were allowed to dry at 22±2 ^{o}C in 40±5% relative humidity for 4 days. Schematic representation of nanostructures and nanocomposites synthesis is shown in Figure 1.

Figure 1

2.2.5. Characterisation

The morphology of titanate nanostructures (e.g., TiNS, STiNS, and TiNT) was examined by Transmission electron microscopy (TEM) (JEOL-3010) and Field emission

scanning electron microscopy (FE-SEM) (JEOL JSM-6500). To prepare TEM samples, a diluted colloidal suspension was dropped on top of a copper grid containing a perforated carbon film and dried for 1 day at 22 ^{o}C. A diluted colloidal suspension of titanate was dropped on top of a silicon wafer for SEM characterisation. For TEM characterisation of the composite samples, the aqueous suspension of titanate nanostructures (e.g., TiNS, STiNS, and TiNT) in the polyamic acid salt was dropped on top of a copper grid with a perforated carbon film and spin coated at 4300 rpm for 1 minute.

Small- and Wide-angle X-ray scattering (SAXS and WAXS) data were collected on a Rigaku SmartLab diffractometer equipped with an in-plane arm and a 9 kW (45 kV, 200 mA) Cu target rotating anode generator. Symmetrical scans were measured in Bragg-Brentano configuration with 5 deg. primary and secondary axial Soller slits and a 1D silicon strip D/teX Ultra 250 detector. In-plane measurements were made in parallel beam configuration with a 0.5 deg. in-plane parallel slit collimator and in-plane parallel slit analyser with the detector operating in 0D mode.

The reduce modulus and hardness were obtained with a Nanotest Platform 3 nanoindenter (Micro Materials Ltd, UK). The conversion method of reduced moduli of the specimens to Young's moduli is provided in Supplementary Information. To prepare the samples, a small cut of the film (around 0.5 cm x 0.5 cm) was glued by epoxy resin to the soda-lime glass with the smoother surface (cast side) on top to be measured. The glass was glued with acrylic to a cylinder holder. The cylinder holder with glass and samples on top was put inside the nanoindenter to be measured using a Berkovich (3-side pyramidal) diamond tip. A constant loading and unloading rate of 20 mN s^{-1} was applied with 30 seconds holding time after reaching the maximum depth. For each samples, 20 indentations at 30 µm intervals were performed at 0.5 mN applied loading.

3. Results and discussion

In the case of carbon nanostructures, it was established that the morphology of the nanostructures (e.g., graphene nanosheets, carbon nanotubes) can affect the reinforcement role in polymer nanocomposites. Graphene outperforms carbon nanotubes in all of the mechanical properties measured, such as Young's modulus, ultimate tensile strength, fracture toughness, fracture energy, and fatigue resistance [32]. Such differences may be caused by better interphase contact between graphene and the polymer matrix as well by differences in dispersion for nanotubes and nanosheets. Graphene has a larger surface area due to a wrinkled surface and enhanced mechanical interlocking. Hence, it is important to study the morphology of titanate nanostructures and evaluate its effect on the mechanical properties of polymer nanocomposites.

3.1. Morphology of titanate nanostructures

The scanning electron microscope (SEM) and transmission electron microscope (TEM) images of TiNS, TiNT, and STiNS are presented in Figure 2.

Figure 2 a,b,c,d,e,f

Nanosheets tend to restack into big platelets when dried, creating a tactoid phase or 'skewed' agglomerates, this makes it difficult to determine their length by SEM (Figure 2a). This type of agglomerate is also observed in clay [33]. Transmission electron microscopy is needed to identify the size of the nanosheets. Due to the extremely thin titanate nanosheets, the nanosheets image shows a very weak contrast [34], making it hard to distinguish the nanostructured material from the background substrate (Figure 2d). Some nanosheets which

stack horizontally on the substrate become more prominent. The colloidal suspension consists mainly of small, irregularly shaped nanosheets particles with a diameter of *ca.* 100 nm. There are some large sheets with a diameter of *ca.* 300 nm together with very small nanotubes (*ca.* 50 nm in length). According to our previous report [10] titanate nanosheets tend to scroll into nanotubes in an alkaline environment. Such scrolling may also occur with very small nanosheets in triethylamine solution.

Hydrothermal treatment of titania in sodium and potassium hydroxides mixed solution at 110 ^{o}C results in formation of titanate nanotubes as seen in Figure 2b. These nanotubes consist of several layers due to the scrolling of layered nanosheets (Figure 2e). The length of nanotubes was reduced from $\approx$150 nm to $\approx$100 nm after ultrasonication while their diameter remained $\approx$25 nm. This result is consistent with previous studies using probe sonication to decrease the length of the titanate nanotubes [13]. The morphology of titanate nanosheets created from hydrothermal synthesis is akin to nanotubes (Figure 2c). Such nanosheets are smaller than the nanotubes with a length of *ca.* 75 nm and diameter of *ca.* 10 nm. Some nanotubes features are distinguishable from a scrolled nanosheets (Figure 2e and 2f). The nanotubes have a defined multi-layered tube structure while scrolled nanosheets have not.

3.2. Effect of settling time (aging) of nanocomposites solution on its mechanical properties

The aging time of mixed aqueous solution of PAAS with nanostructured titanate affects the mechanical properties of final composite. The samples with longer settling time had inferior properties. During aging, the coagulation of nanostructures into large agglomerates occurs. In the case of carbon nanotubes, agglomeration may appear in the liquid

epoxy resin during curing, even at a low filler content (0.05 wt%) [35]. In this work, the settling time to synthesise nanocomposites was varied. After stirring the composite mixture for 3 days, samples were either used immediately or settled for one week. Agglomeration occurred on the sample after one week settling time (Figure 3).

Figure 3

This agglomeration resulted in to 27.35% reduction of the modulus from 3.51±0.20 GPa to 2.55±0.12 GPa for TiNT samples with and without and with agglomerates respectively. For scrolled titanate nanosheets (STiNS) samples it reduced by 27.91% from 3.26±0.17 GPa to 2.35±0.14 GPa. While for TiNS samples the modulus decreases by 22.83% from 4.03±0.13 GPa to 3.11±0.43 GPa. Thermodynamically, such a colloidal suspension is unstable since nanostructures (TiNS, TiNT, STiNS) [10,36] and polymer, both, have a negative surface charge [37]. However, the kinetic stability of the suspension allows a good dispersion of nanostructures within the polymer matrix, if a short aging time is used. This agglomeration also occurs when the filler concentration (e.g., TiNS, TiNT, STiNS) is more than 2 wt%, probably due to stronger van der Waals interaction in densely packed nanostructures.

3.3. Effect of titanate nanosheets (TiNS) on mechanical properties of water-soluble polymers

In order to study the synthetic method for nanocomposites, comparison of experimental results with existing theoretical prediction is necessary. Herein, we used titanate nanosheets (TiNS) as filler of polymer nanocomposites using solution processing synthesis methods. Figure 4a and 4b shows experimental data and theoretical predictions of the

hardness and modulus of titanate nanosheets-polyamic acid salt nanocomposites with different concentrations of TiNS (0, 0.5, 1, 2, 3, 5 wt%).

Figure 4 a,b

The addition of titanate nanosheets significantly enhanced the hardness and modulus of the water-soluble polyamic acid salt. The hardness increased 90% with addition of 2% TiNS, while the modulus increased 103% compared to the pure polymer. The improvement in hardness matched the Halpin-Tsai theory up to 2 wt% while, for the modulus, it followed up to 1 wt%. It also followed the modified rule of mixtures with a 0.8 particle strengthening factor for hardness, which is a factor determined empirically, up to 2 wt%. For the modulus, it corresponded up to 1 wt% to a 0.6 particle strengthening factor of modified rule of mixtures.

Figure 5 a, b, c

Beyond the critical concentration (2 wt%), experimental results are not correlated with predictions. This might happen because at low filler concentrations the nanosheets are fully exfoliated (Figure 5a) maintaining the same aspect ratio and polymer-filler interactions. At higher filler loading, ‘skewed’ platelets or tactoid phases are created (Figure 5b). Severe agglomerations may act as stress concentration sites [18]. (010) and (020) peaks shift to the left in SAXS patterns of TiNS sample and 5 wt% TiNS-PAAS (Figure 5c). This shows that the interlayer distance of nanosheets is increased from 7.22 Å to 9.09 Å due to intercalation of the polymer. The disappearance of peaks at low concentration of TiNS (0.5 wt%) may be caused by exfoliation of TiNS within the polyamic acid.

The number of stacked nanosheets and the correlation with the mechanical properties may also be predicted using the Brune-Bicerano model [38]. This model assumes the

nanosheets are stacked in parallel and all platelets which contain the same number of stacks are dispersed unidirectionally within the polymer. The equation is as follows:

$$\frac{E_c}{E_m} = \frac{1+2A'_f\eta'\phi'}{1-\eta'\phi'} \quad (7)$$

$$\eta' = \frac{E'_f-1}{E'_f+2A'_f} \quad (8)$$

$$A'_f = \frac{A_f}{N'}\left(\frac{1}{1+(1-1/N')\frac{s}{t}}\right) \quad (9)$$

$$\phi' = \phi\,(1+(1-1/N')\frac{s}{t}) \quad (10)$$

$$E'_f = E_f\left(\frac{1}{1+(1-1/N')\frac{s}{t}}\right) + \frac{(1-1/N')\frac{s}{t}}{1+(1-1/N')\frac{s}{t}} \quad (11)$$

$$N' = N + (1-1/N)\frac{s}{t}\left(\frac{\phi}{1-\phi}\right) \quad (12)$$

where E_c, E_m, and E_f are moduli of the composite, the matrix and TiO_2 (taken from literature [24]) respectively. A_f is the aspect ratio of the filler (l/h) where l is the nanosheets length and h is the nanosheets thickness. Φ is the filler volume fraction and N is number of stacks. s/t is the ratio of spacing between nanosheets to thickness of a nanosheet. The spacing is determined by SAXS measurements (9.09 Å, Figure 5c) and the geometry of the nanosheets (e.g., length and thickness) is evaluated by TEM (Figure 5a). Hardness is predicted by substituting the modulus with hardness.

Figure 6 a,b

Figure 6 shows the experimental and theoretical predictions of the modulus and hardness of nanocomposites for incomplete exfoliation. The modulus and hardness of nanocomposites fit the Brune-Bicerano model for 3 stacks at 2 wt% of TiNS. A 3 stack

aggregate of nanosheets may impede the modulus and hardness improvement at 2 wt% of TiNS. The Halpin-Tsai and Halpin-Kardos models cannot accurately predict the mechanical properties when there is incomplete exfoliation (Figure 4a and 4b). The Brune-Bicerano prediction is not accurate at relatively high filler content having a higher number of stacks. This model suggests that at 3 wt% and 5 wt% of TiNS, 50 stacks of TiNS may occur as fitted in the model, while TEM images in Figure 5b show that the agglomerates have fewer than 50 stacks. At high content, the nanosheets agglomerate not only in parallel but also horizontally creating 'skewed' structures which are observed by TEM (Figure 5b). This model should thus be evaluated taking into account the horizontal stacks.

Figure 7 a, b

In Figure 7, small-angle x-ray scattering (SAXS) shows that the (010) and (020) basal spacing of titanate nanosheets [39], which is 9.09 Å (d_{010}) and 17.88 Å (d_{020}), are not observed in the in-plane direction to the sample surface (in-plane scan) while in parallel direction (symmetric scan) these peaks are detected (Figure 7a). A homogeneous preferred orientation is also observed in the nanocomposite film proven by mapping across 18 spots on the sample (Figure 7b). This proves that the titanate nanosheets were homogeneously aligned parallel to the surface inside the polymer (perpendicular to the indentation loading). This correlates with the Halpin-Tsai theory which assumes that the filler is unidirectional. This orientation is beneficial since titanate nanosheets have anisotropic reinforcement which is highest when the loading is perpendicular to the nanosheets [4]. In the case of clay, shearing (e.g., doctor blade) is required to induce preferred orientation of the clay within the polymer matrix [40]. For titanate nanosheets, simple drop casting produces oriented nanosheets within the polymer.

3.4. Effect of titanate nanotubes (TiNT) and scrolled titanate nanosheets (STiNS) on mechanical properties of water-soluble polymers

Figure 8a and 8b show experimental data and theoretical predictions of hardness and modulus of the titanate nanotubes-polyamic acid salt (TiNT-PAAS) nanocomposites with different concentrations of TiNS (0, 0.5, 1, 2, 3, 5 wt%).

Figure 8 a,b

The hardness and modulus of the polyamic acid salt increased 91% and 165% by incorporation of 2 wt% titanate nanotubes respectively. This improvement was reduced and became stagnant after 2 wt% loading of titanate nanotubes. At 3 and 5 wt% TiNT, the improvement for the modulus was 104% and 108% respectively. This reinforcement tendency is similar to that in previously reported studies [13] also using ultrasonication to disperse the nanotubes. Shorter nanotubes are formed due to sonication leading to reduction of their mechanical properties [41]. It may also accelerate the dispersion of the nanotubes [42] and hence the mechanical properties of TiNT-PAAS nanocomposites were increased. However, aggregation of nanotubes may happen at high concentrations reducing the reinforcement effect of nanotubes. There was no difference in SAXS profile when the film was measured in either out-of-plane or in-plane directions (Figure S1). This proves that titanate nanotubes were dispersed randomly with no preferred orientation.

At low TiNT content (<3 wt%), the experimental data correspond to the modified rule of mixtures with a 0.8 particle strengthening factor for hardness and 0.6 for the modulus. Halpin-Tsai and Halpin-Kardos predictions, using TiO_2 filler properties, underestimated the mechanical properties of nanocomposites which may indicate that hydrothermal titanate nanotubes structure, which is akin to $H_2Ti_3O_7$ [43,44], is stronger than bulk TiO_2. Currently, studies on the mechanical properties of titanate nanotubes mainly focus on anodized titanate

nanotubes [45,46] which are single nanotubes with moduli ranging from 2.2 to 9.4 GPa. This number is much lower than the modulus of TiO_2 (282.76 GPa). Therefore, comprehensive studies on the mechanical properties of hydrothermally synthesised titanate nanotubes are needed in the future. It can be done experimentally using atomic force microscopy [47], micro-Raman [48] and TEM [49] observation of thermally induced stress, or theoretically [50-54]. SAXS profiles of the titanate nanotubes and scrolled nanosheets are provided in Figure 9.

Figure 9

Scrolled titanate nanosheets have a similar structure to titanate nanotubes and the only difference in the SAXS profile is in the peaks at low angle. These peaks correspond to interlayer spacing of multi-layered nanotubes in the radial direction, which is not apparent in incomplete scrolling of nanosheets (scrolled titanate nanosheets only scroll on the edges). This supports the scrolling mechanism of titanate nanotubes during synthesis which argues that nanotubes are formed from scrolling of sheets [55].

Figure 10a and 10b give the nanoindentation results and predictions of scrolled titanate nanosheets-polyamic acid salt (STiNS-PAAS) nanocomposites with controlled concentrations of STiNS (0, 0.5, 1, 2, 3, 5 wt%).

Figure 10a and b

Although STiNS and TiNT have the same structures (Figure 9), their reinforcement behaviour is different. The mechanical improvement of nanocomposites skewed until it reached 3 wt%. The modulus improved by 104% and 97% for 3 and 5 wt% of STiNS respectively. This skewed improvement is probably caused by the less defined structured of

STiNS which is an intermediate structure between sheet and tube. The experimental results were also higher than Halpin-Tsai and Halpin-Kardos predictions, which using TiO_2 as filler properties, proving that hydrothermal titanate has higher mechanical properties than TiO_2. It followed the modified rule of mixtures with a 0.3 particle strengthening factor for the hardness and 0.2 for the modulus. Higher reinforcement behaviour of nanostructures (TiNS, TiNT, and STiNS) reflected in higher number of the hardness particle strengthening factors which are 0.8, 0.8, 0.3 for TiNS, TiNT, and STiNS respectively. The high reinforcement ability of TiNS may be due to preferred orientation of nanosheets within matrix thus optimizing the reinforcement. Unlike TiNS, hydrothermal TiNT and STiNS have random orientation. Their reinforcement may be caused by high mechanical properties of hydrothermally synthesised titanate nanostructures. However, scrolled titanate nanosheets (STiNS) may also have anisotropic mechanical properties like TiNS [4], that significantly lowering the mechanical properties of STiNS-PAAS nanocomposite, which has random orientation instead of arranged unidirectionally.

4. Conclusions

Titanate nanosheets, titanate nanotubes, and scrolled titanate nanosheets are used in this work to improve the mechanical properties of the polyamic acid salt. Settling time in nanocomposite processing is also studied and shorter settling time is preferable to avoid agglomeration. Addition of titanate nanosheets to water soluble polyamic acid significantly enhances the hardness and modulus of the polymer. The hardness increases by 90% on addition of 2% TiNS while the modulus increases by 103% compared to the pure polymer. This proves that triethylamine (TEA) can be used as a bulky molecule instead of tetrabutyl ammonium hydroxide (common chemical for titanate nanosheets exfoliation) to exfoliate

titanate nanosheets. A high aspect ratio (l/h = 133.33) and uniform distribution of titanate nanosheets provides significant reinforcement of polymer. Dispersed nanosheets aligned within the polymer matrix (parallel to the surface) were observed by SAXS. This reinforcement behaviour matches well with Halpin-Tsai theory [16] at low filler content (up to 1 wt%) assuming the filler has a unidirectional orientation. At 2 wt% of TiNS it followed the Brune-Bicerano model with 3 stacks of nanosheets agglomerates. At high filler loadings (>2 wt%), the mechanical properties of the composites did not fit established theories due to 'skewed' agglomeration of the titanate nanosheets. These sheets are stacked on each other, creating several layers of elongated agglomerates. This causes poor distribution of nanosheets and might disturb the stress distribution between nanosheets and the polymer. This elongated agglomerate suggests improvement of the Brune-Bicerano model [38] which only considers sheets stacking in a parallel direction.

Although titanate nanotubes have a lower aspect ratio (l/h = 4) and random orientation, they have a higher reinforcement ability. The hardness and modulus of the polyamic acid salt increased 91% and 165% by addition of 2 wt% titanate nanotubes respectively. This indicates that titanate nanotubes made by hydrothermal synthesis may have higher mechanical properties than bulk TiO_2. However, the mechanical properties of nanocomposites reached a plateau after 2 wt% of TiNT due to aggregation of TiNT. Higher reinforcement effectiveness of the nanostructures can be represented by higher value of the hardness particle strengthening factors of the nanostructures (TiNS, TiNT, and STiNS), which are 0.8, 0.8, 0.3 for TiNS, TiNT, and STiNS respectively. Whereas having different structure, it is possible that the hydrothermally synthesised scrolled titanate nanosheets (STiNS) have anisotropic mechanical properties such as titanate nanosheets (TiNS) made by exfoliation of solid state reaction [4], lowering the reinforcement ability on the polymer matrix when dispersed randomly within the matrix.

Figure captions (colour should be used for all figures)

Figure 1 Schematic representation for the synthesis of titanate nanosheets (TiNS), titanate nanotubes (TiNT), scrolled titanate nanosheets (STINS) and their composites with polyamic acid salt (PAAS).

Figure 2 SEM images (a), (b), (c) and TEM images (d), (e), (f) of titanate nanosheets, titanate nanotubes, and scrolled titanate nanosheets, respectively

Figure 3 TEM images showing agglomeration of (a) titanate nanotubes; (b) titanate nanosheets

Figure 4 Nanoindentation data of titanate nanosheets-polyamic acid salt (TiNS-PAAS) nanocomposites compared to Halpin-Tsai, Halpin-Kardos, modified rule of mixture (ROM) theories; (a) hardness; (b) modulus

Figure 5 TEM images showing (a) exfoliated; (b) aggromerated titanate nanosheets (TiNS); (c) combined SAXS & WAXS profile of (i) TiNS only, (ii) polymer intercalated TiNS at 5 wt% of TiNS (peaks shifted to the left indicating larger interlayer distance of nanosheets), (iii) exfoliated TiNS at 0.5 wt% of TiNS (no peaks detected proving that the sample containing single layer sheets)

Figure 6 Comparison of nanoindentation data of titanate nanosheets-polyamic acid salt (TiNS-PAAS) with Brune-Bicerano model with various numbers of stacks (N); (a) hardness; (b) modulus

Figure 7 Combined SAXS & WAXS profile proving orientation of titanate nanosheets (TiNS) within polymer (a) TiNS peaks detected by symmetric scan (red, i) while it disappeared in in-plane scan (black, ii); (b) SAXS profile data of 18 samples symmetric scan with 1 mm apart

(shown in inset) was provided, slight variation of peaks and intensity occur due to the sample was not perfectly flat.

Figure 8 Nanoindentation data of titanate nanotubes-polyamic acid salt (TiNT-PAAS) nanocomposites compared to Halpin-Tsai, Halpin-Kardos, modified rule of mixture (ROM) theories; (a) hardness; (b) modulus.

Figure 9 Combined SAXS & WAXS profile of (a) titanate nanotubes (TiNT); (b) scrolled titanate nanosheets (STiNS). (010) peak is visible in titanate nanotubes sample.

Figure 10 Nanoindentation data of scrolled titanate nanosheets-polyamic acid salt (STiNS-PAAS) nanocomposites compared to Halpin-Tsai, Halpin-Kardos, modified rule of mixture (ROM) theories; (a) hardness; (b) modulus.

Figure S1 Combined SAXS & WAXS measurement for 5 wt% titanate nanotubes within polymer (a) symmetric scan (red); (b) in-plane scan (black). Neither shows any significant peaks due to alignment. In-plane scans are always of much lower intensity.

Acknowledgements

The authors are grateful for the funding from Indonesian Endowment Fund for Education (LPDP) and the EPSRC for financial support of equipment grant (EP/K00509X/1) for the SmartLab.

References

[1] Yoshitsugu K, Arimitsu U, Masaya K, Akane O, Yoshiaki F, Toshio K, Kamigaito O. Mechanical properties of nylon 6-clay hybrid. J Mater Res 1993;8;1185–9.

[2] Sasaki T, Watanabe M. Osmotic swelling to exfoliation. Exceptionally high degrees of hydration of a layered titanate. J Am Chem Soc 1998;120;4682–9. doi:10.1021/ja974262l.

[3] Wang L, Sasaki T. Titanium oxide nanosheets: graphene analogues with versatile functionalities. Chem Rev 2014;114;9455–86. doi:10.1021/cr400627u.

[4] Liu M, Ishida Y, Ebina Y, Sasaki T, Aida T. Photolatently modulable hydrogels using unilamellar titania nanosheets as photocatalytic crosslinkers. Nat Commun 2013;4;743–56. doi:10.1038/ncomms3029.

[5] Marani D, D'Epifanio A, Traversa E, Miyayama M, Licoccia S. Titania nanosheets (TNS)/sulfonated poly ether ether ketone (SPEEK) nanocomposite proton pxchange membranes for fuel cells. Chem Mater 2010;22;1126–33. doi:10.1021/cm902405p.

[6] Ratanatawanate C, Perez M, Gnade BE, Balkus KJ. Layer-by-layer assembly of titanate nanosheets/poly- (ethylenimine) on PEN films. Mater Lett 2012;66;242–5. doi:10.1016/j.matlet.2011.08.089.

[7] Bavykin DV, Kulak AN, Walsh FC. Metastable nature of titanate nanotubes in an alkaline environment. Cryst Growth Des 2010;10;4421–7. doi:10.1021/cg100529y.

[8] Kasuga T, Hiramatsu M, Hoson A, Sekino T, Niihara K. Formation of titanium oxide nanotubes. Langmuir 1998;14;3160–3. doi:10.1021/LA9713816.

[9] Sumisha A, Arthanareeswaran G, Ismail AF, Kumar DP, Shankar MV. Functionalized

titanate nanotubes–polyetherimide nanocomposite membrane for improved salt rejection under low pressure nanofiltration. RSC Adv. 2015;5;39464–73. doi:10.1039/C5RA03520A.

[10] Bavykin DV, Friedrich JM, Walsh FC. Protonated titanates and TiO_2 nanostructured materials: synthesis, properties, and applications. Adv. Mater 2006;18;2807–24. doi:10.1002/adma.200502696.

[11] Herrasti P, Kulak AN, Bavykin DV, de Léon CP, Zekonyte J, Walsh FC. Electrodeposition of polypyrrole–titanate nanotubes composites coatings and their corrosion resistance. Electrochim Acta 2011;56;1323–8. doi:10.1016/j.electacta.2010.09.094.

[12] Harito C, Porras R, Bavykin DV, Walsh FC. Electrospinning of *in-situ* and *ex-situ* synthesized polyimide composites reinforced by titanate nanotubes. J Appl Polym Sci 2016;133;44641. doi:10.1002/app.44641.

[13] Porras R, Bavykin DV, Zekonyte J, Walsh FC, Wood RJ. Titanate nanotubes for reinforcement of a poly(ethylene oxide)/chitosan polymer matrix. Nanotechnology 2016;27;195706. doi:10.1088/0957-4484/27/19/195706.

[14] Cai D, Su J, Huang M, Liu Y, Wang J, Dai L. Synthesis, characterization and hydrolytic stability of poly (amic acid) ammonium salt. Polym Degrad Stab 2011;96;2174–80. doi:10.1016/j.polymdegradstab.2011.09.008.

[15] Fu S-Y, Xu G, Mai Y-W. On the elastic modulus of hybrid particle/short-fiber/polymer composites. Compos Part B - Eng 2002;33;291–9. doi:10.1016/S1359-8368(02)00013-6.

[16] Halpin JC. Stiffness and expansion estimates for oriented short fiber composites. J

Compos Mater 1969;3;732–4. doi:10.1177/002199836900300419.

[17] Halpin JC, Kardos JL. The Halpin-Tsai equations: a review. Polym Eng Sci 1976;16;344–52. doi:10.1002/pen.760160512.

[18] Ebadi-Dehaghani H, Khonakdar HA, Barikani M, Jafari SH. Experimental and theoretical analyses of mechanical properties of PP/PLA/clay nanocomposites. Compos Part B - Eng 2015;69;133–44. doi:10.1016/j.compositesb.2014.09.006.

[19] Shiu S-C, Tsai J-L. Characterizing thermal and mechanical properties of graphene/epoxy nanocomposites. Compos Part B - Eng 2014;56;691–7. doi:10.1016/j.compositesb.2013.09.007.

[20] Gupta AK, Harsha SP. Analysis of mechanical properties of carbon nanotubes reinforced polymer composites using multi-scale finite element modeling approach, Compos. Part B - Eng 2016;95;172–8. doi:10.1016/j.compositesb.2016.04.005.

[21] Voigt W. Ueber die beziehung zwischen den beiden elasticitätsconstanten isotroper körper. Ann Phys 1889;274;573–87. doi:10.1002/andp.18892741206.

[22] Nielsen LE, Landel RF. Mechanical properties of polymers and composites. M. Dekker, 1994.

[23] Lewis TB, Nielsen LE. Dynamic mechanical properties of particulate-filled composites. J Appl Polym Sci 1970;14;1449–71. doi:10.1002/app.1970.070140604.

[24] Shackelford JF, Alexander W. Mechanical properties of materials, in: Shackelford JF, Alexander W (Eds.), CRC Mater. Sci. Eng. Handbook, Third Ed., 3rd ed., CRC Press, 2000. doi:doi:10.1201/9781420038408.ch6.

[25] Bokobza L. Multiwall carbon nanotubes elastomeric composites: a review. Polymer

2007;48;4907–20. doi:10.1016/j.polymer.2007.06.046.

[26] Wan C, Chen B. Reinforcement and interphase of polymer/graphene oxide nanocomposites. J Mater Chem 2012;22;3637–46. doi:10.1039/c2jm15062j.

[27] Goyal RK, Tiwari AN, Negi YS. Microhardness of PEEK/ceramic micro- and nanocomposites: correlation with Halpin–Tsai model. Mater Sci Eng A 2008;491;230–6. doi:10.1016/j.msea.2008.01.091.

[28] Sasaki T, Watanabe M. Osmotic swelling to exfoliation. Exceptionally high degrees of hydration of a layered titanate. J Am Chem Soc 1998;120;4682–9. doi:10.1021/JA974262L.

[29] Grey IE, Li C, Madsen IC, Watts JA. The stability and structure of $Cs_x[Ti_{2-x/4}\square_{x4}]O_4$, $0.61 < x < 0.65$. J Solid State Chem 1987;66;7–19. doi:10.1016/0022-4596(87)90215-5.

[30] Lee T, Park SS, Jung Y, Han S, Han D, Kim I, Ha C-S. Preparation and characterization of polyimide/mesoporous silica hybrid nanocomposites based on water-soluble poly(amic acid) ammonium salt. Eur Polym J 2009;45;19–29. doi:10.1016/j.eurpolymj.2008.09.022.

[31] Kreuz JA, Endrey AL, Gay FP, Sroog CE. Studies of thermal cyclizations of polyamic acids and tertiary amine salts. J Polym Sci Part A-1 Polym Chem 1966;4;2607–16. doi:10.1002/pol.1966.150041023.

[32] Rafiee MA, Rafiee J, Wang Z, Song H, Yu Z-Z, Koratkar N. Enhanced mechanical properties of nanocomposites at low graphene content. ACS Nano. 2009;3;3884–90. doi:10.1021/nn9010472.

[33] Paul DR, Robeson LM. Polymer nanotechnology: nanocomposites. Polymer 2008;49;3187–204. doi:10.1016/j.polymer.2008.04.017.

[34] Sasaki T, Ebina Y, Kitami Y, Watanabe M, Oikawa T. Two-dimensional diffraction of molecular nanosheets crystallites of titanium oxide. J Phys Chem B 2001;105;6116–21. doi:10.1021/JP010421I.

[35] Ma P-C, Mo S-Y, Tang B-Z, Kim J-K. Dispersion, interfacial interaction and re-agglomeration of functionalized carbon nanotubes in epoxy composites. Carbon 2010;48; 1824–34. doi:10.1016/j.carbon.2010.01.028.

[36] Osada M, Sasaki T. Nanosheets architectonics: a hierarchically structured assembly for tailored fusion materials. Polym J 2015; 47;89–98. doi:10.1038/pj.2014.111.

[37] Ding F, Tong Y, Luo X, Guan H, Hu B. Preparation, characterization, and properties of polyamic acid nano-emulsion. Polym Adv Technol 2011;22;2633–7. doi:10.1002/pat.1913.

[38] Brune DA, Bicerano J. Micromechanics of nanocomposites: comparison of tensile and compressive elastic moduli, and prediction of effects of incomplete exfoliation and imperfect alignment on modulus. Polymer 2002;43;369–87. doi:10.1016/S0032-3861(01)00543-2.

[39] Kim TW, Kim IY, Park D-H, Choy J-H, Hwang S-J. Highly stable nanocontainer of APTES-anchored layered titanate nanosheets for reliable protection/recovery of nucleic acid. Sci Rep 2016;6;21993. doi:10.1038/srep21993.

[40] Malwitz MM, Lin-Gibson S, Hobbie EK, Butler PD, Schmidt G. Orientation of platelets in multilayered nanocomposite polymer films. J Polym Sci Part B Polym Phys 2003;41;3237–48. doi:10.1002/polb.10699.

[41] Arash B, Wang Q, Varadan VK. Mechanical properties of carbon nanotubes/polymer composites. Sci Rep 2014;4;6479. doi:10.1038/srep06479.

[42] Qian D, Dickey EC, Andrews R, Rantell T. Load transfer and deformation mechanisms in carbon nanotubes-polystyrene composites. Appl Phys Lett 2000;76;2868–70. doi:10.1063/1.126500.

[43] Chen Q, Du GH, Zhang S, Peng L-M. The structure of trititanate nanotubes. Acta Crystallogr B 2002;58;587–93. doi:10.1107/S0108768102009084.

[44] Du GH, Chen Q, Che RC, Yuan ZY, Peng L-M. Preparation and structure analysis of titanium oxide nanotubes. Appl Phys Lett 2001;79;3702. doi:10.1063/1.1423403.

[45] Kang S-H, Fang T-H, Chen T-H, Hsiao Y-J, Hong Z-H, Chuang C-H, Riccobono L. Size effect on mechanical properties of TiO_2 capped nanotubes investigated using in situ transmission electron microscopy. Microsyst Technol 2014;20;515–20. doi:10.1007/s00542-013-1939-0.

[46] Shokuhfar T, Arumugam GK, Heiden PA, Yassar RS, Friedrich C. Direct compressive measurements of individual titanium dioxide nanotubes. ACS Nano 2009;3;3098–102. doi:10.1021/nn900202x.

[47] Salvetat J-P, Bonard J-M, Thomson NH, Kulik AJ, Forró L, Benoit W, Zuppiroli L. Mechanical properties of carbon nanotubes. Applied Physics A 1999;69;255-60. doi: 10.1007/s003399900114

[48] Lourie O, Wagner HD. Evaluation of Young's modulus of carbon nanotubes by micro-Raman spectroscopy. Journal of Materials Research 1998;13;2418-22. doi: 10.1098/rspa.1990.0045

[49] Treacy MMJ, Ebbesen TW, Gibson JM. Exceptionally high Young's modulus observed for individual carbon nanotubes. Nature 1996;381;678-80. doi: 10.1038/381678a0

[50] Barretta R, Feo L, Luciano R, Marotti de Sciarra F. An Eringen-like model for Timoshenko nanobeams. Composite Structures 2016;139;104-10. doi: 10.1016/j.compstruct.2015.11.048

[51] Barretta R, Feo L, Luciano R, Marotti de Sciarra F. Application of an enhanced version of the Eringen differential model to nanotechnology. Composites Part B: Engineering 2016;96;274-80. doi: 10.1016/j.compositesb.2016.04.023

[52] Barretta R, Feo L, Luciano R, Marotti de Sciarra F, Penna R. Functionally graded Timoshenko nanobeams: a novel nonlocal gradient formulation. Composites Part B: Engineering 2016;100;208-19. doi: 10.1016/j.compositesb.2016.05.052

[53] Romano G, Barretta R. Stress-driven versus strain-driven nonlocal integral model for elastic nano-beams. Composites Part B: Engineering 2017;114;184-8. doi: 10.1016/j.compositesb.2017.01.008

[54] Apuzzo A, Barretta R, Canadija M, Feo L, Luciano R, Marotti de Sciarra F. A closed-form model for torsion of nanobeams with an enhanced nonlocal formulation. Composites Part B: Engineering 2017;108;315-24. doi: 10.1016/j.compositesb.2016.09.012

[55] Bavykin DV, Parmon VN, Lapkin AA, Walsh FC. The effect of hydrothermal conditions on the mesoporous structure of TiO_2 nanotubes. J Mater Chem 2004;14;3370. doi:10.1039/b406378c.

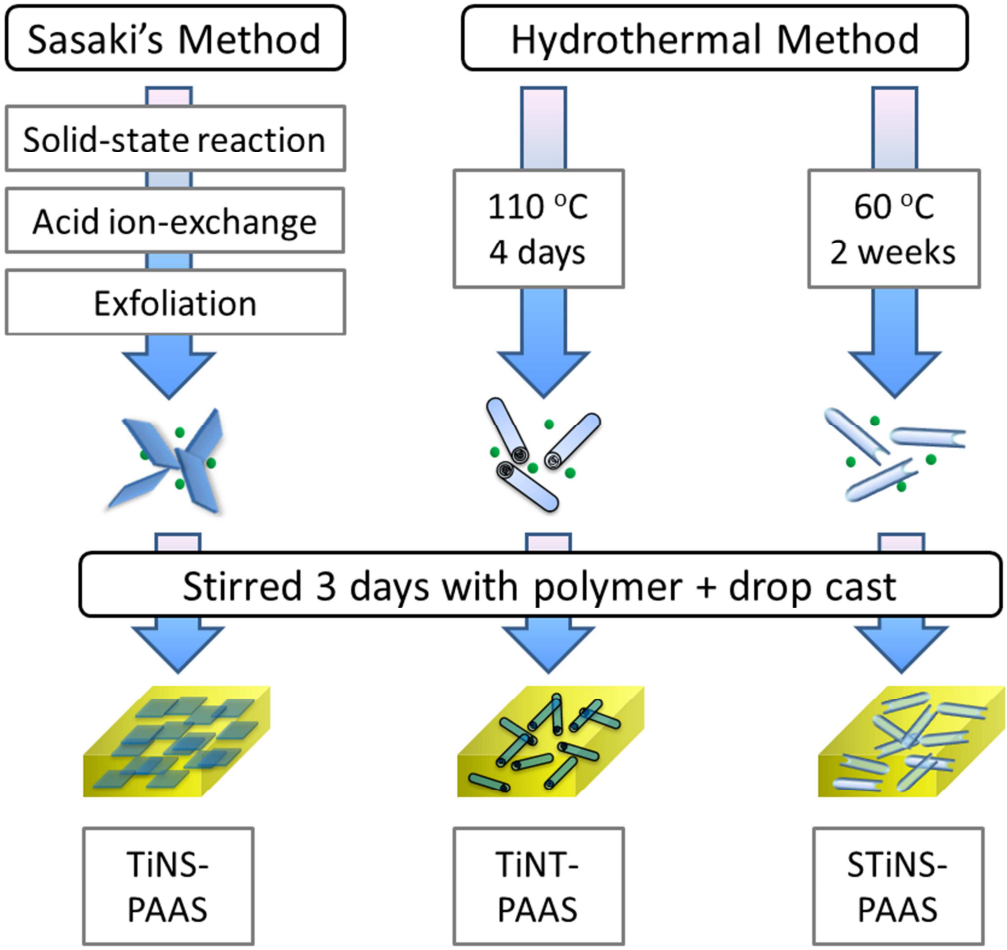

Figure 1

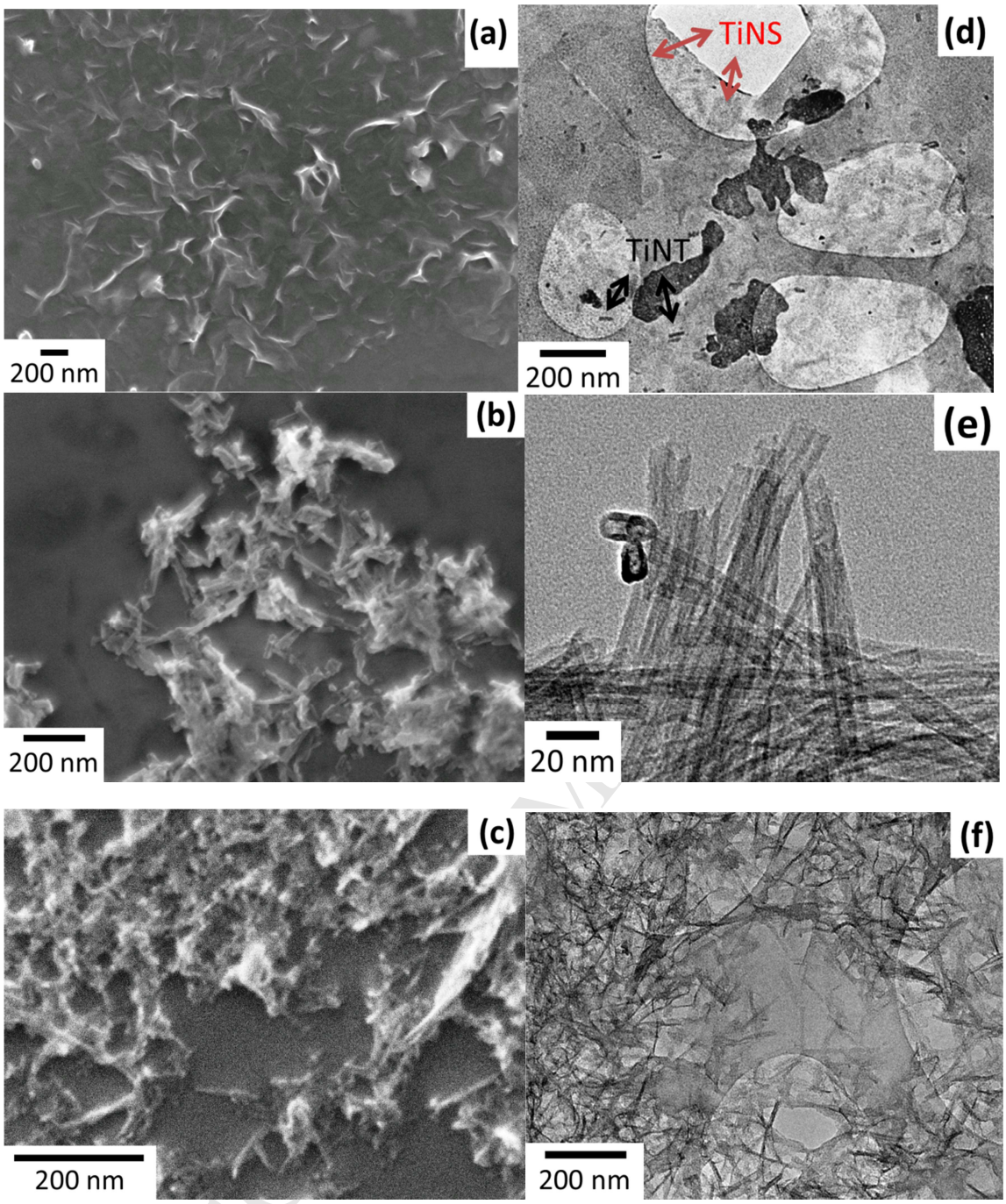

Figure 2

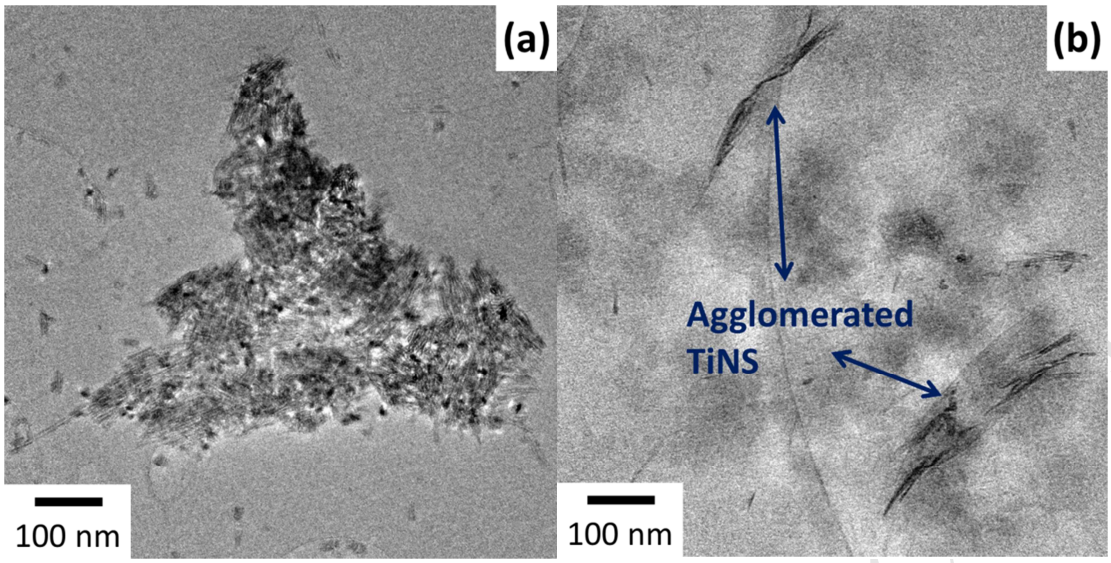

Figure 3

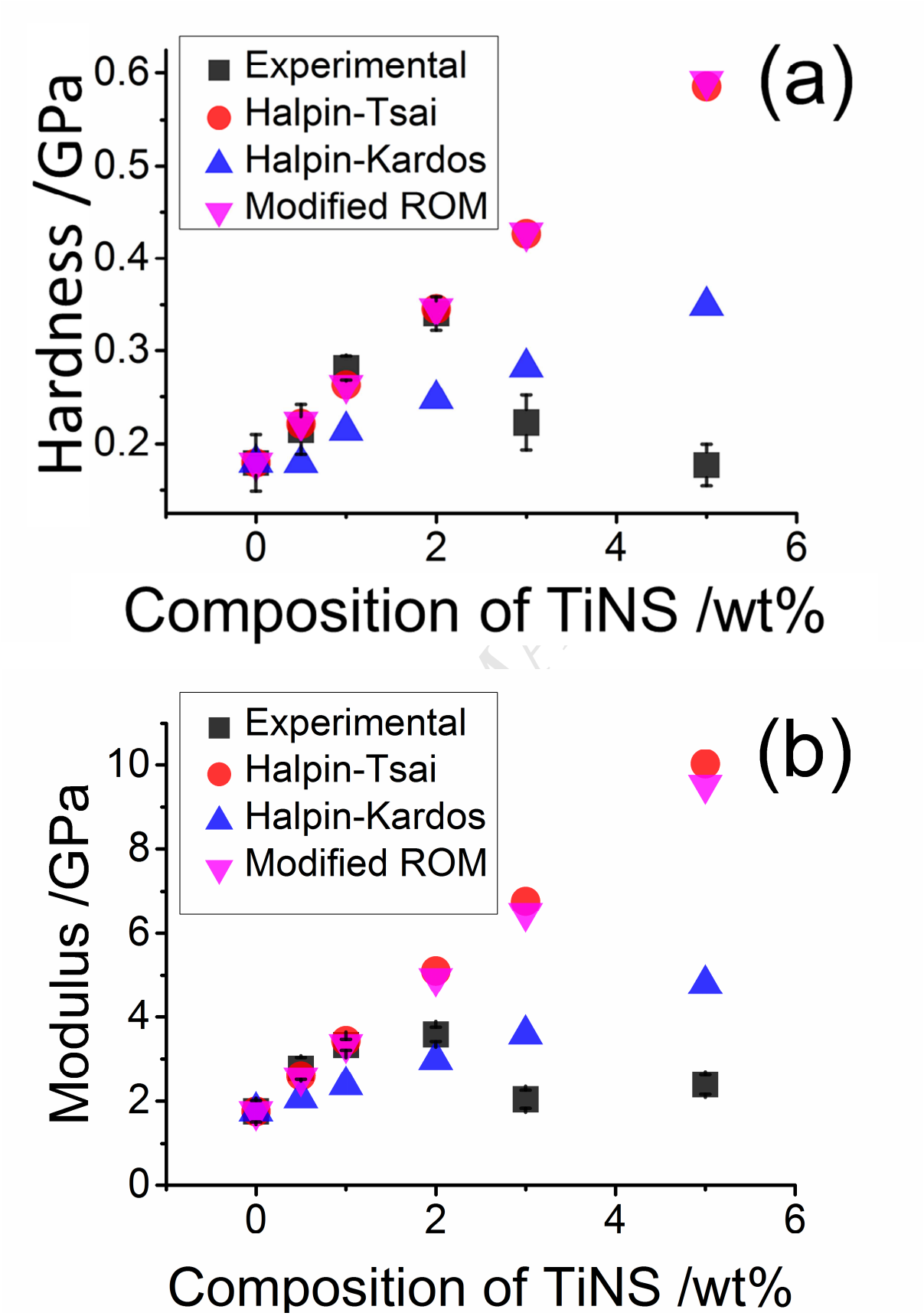
Experimental
Halpin-Tsai
Halpin-Kardos
Modified ROM
(a)
Hardness /GPa
0.2
0.3
0.4
0.5
0.6
0
2
4
6
Composition of TiNS /wt%
Experimental
Halpin-Tsai
Halpin-Kardos
Modified ROM
(b)
Modulus /GPa
0
2
4
6
8
10
0
2
4
6
Composition of TiNS /wt%

Figure 4

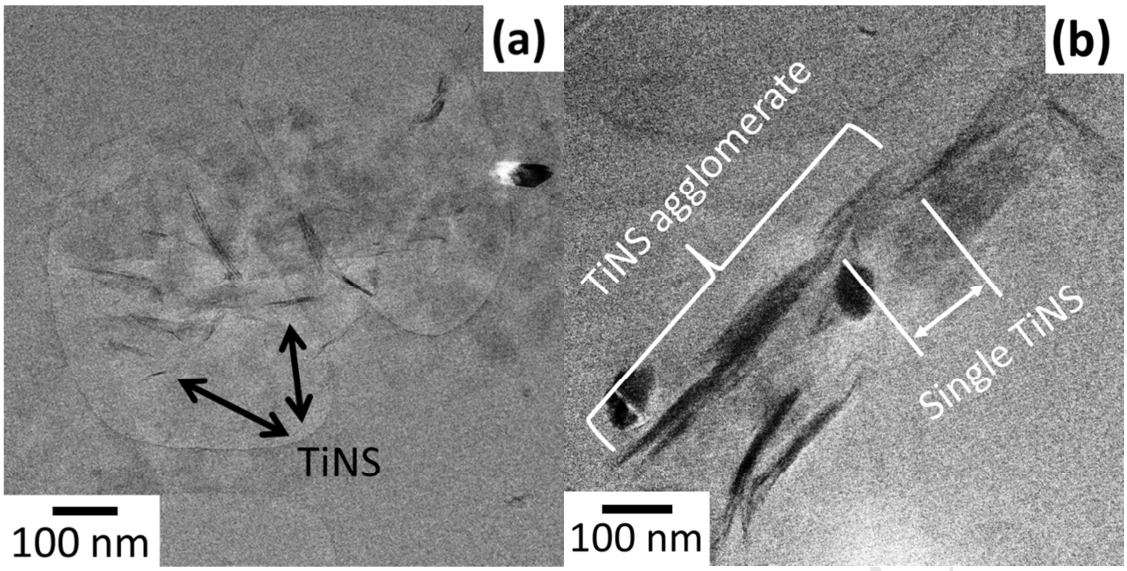
(a)
TiNS
100 nm
(b)
TiNS agglomerate
Single TiNS
100 nm

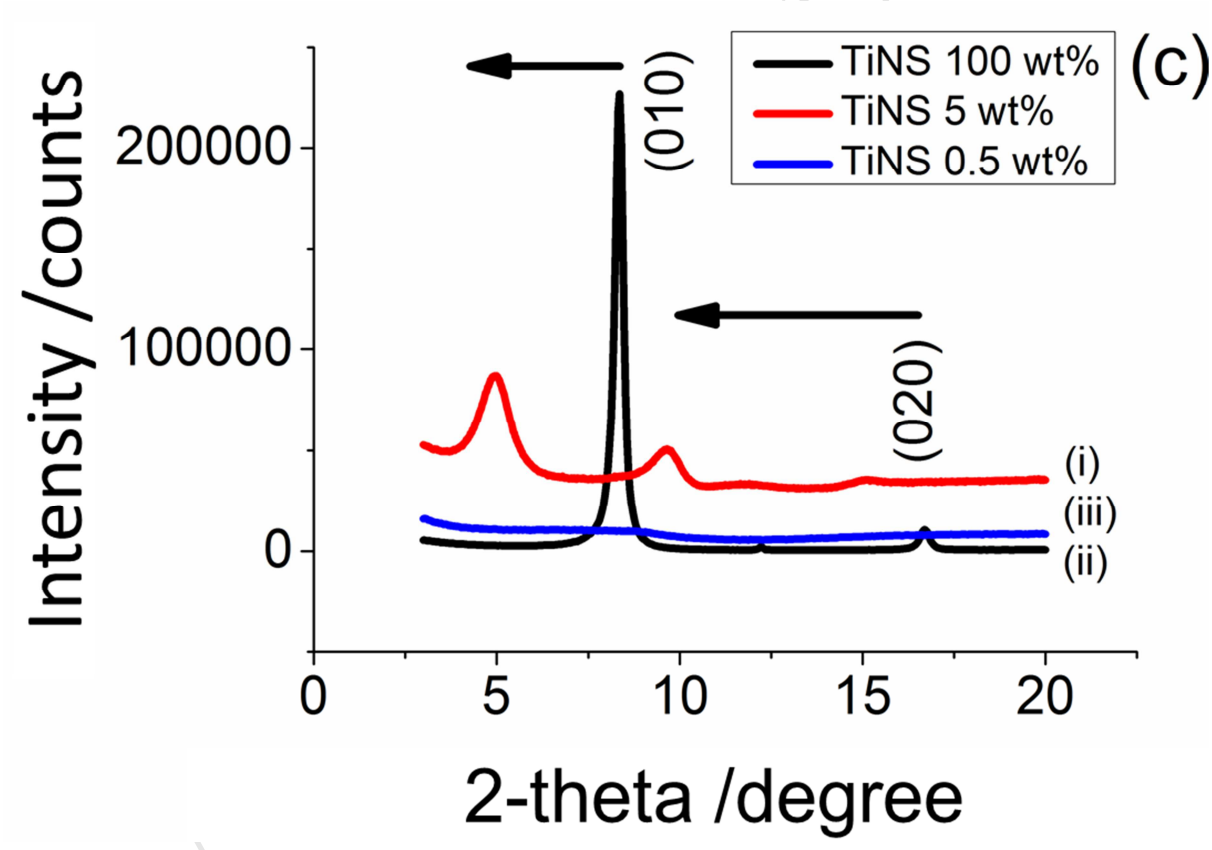
(c)
TiNS 100 wt%
TiNS 5 wt%
TiNS 0.5 wt%
(010)
(020)
(i)
(iii)
(ii)
Intensity /counts
200000
100000
0
0
5
10
15
20
2-theta /degree

Figure 5

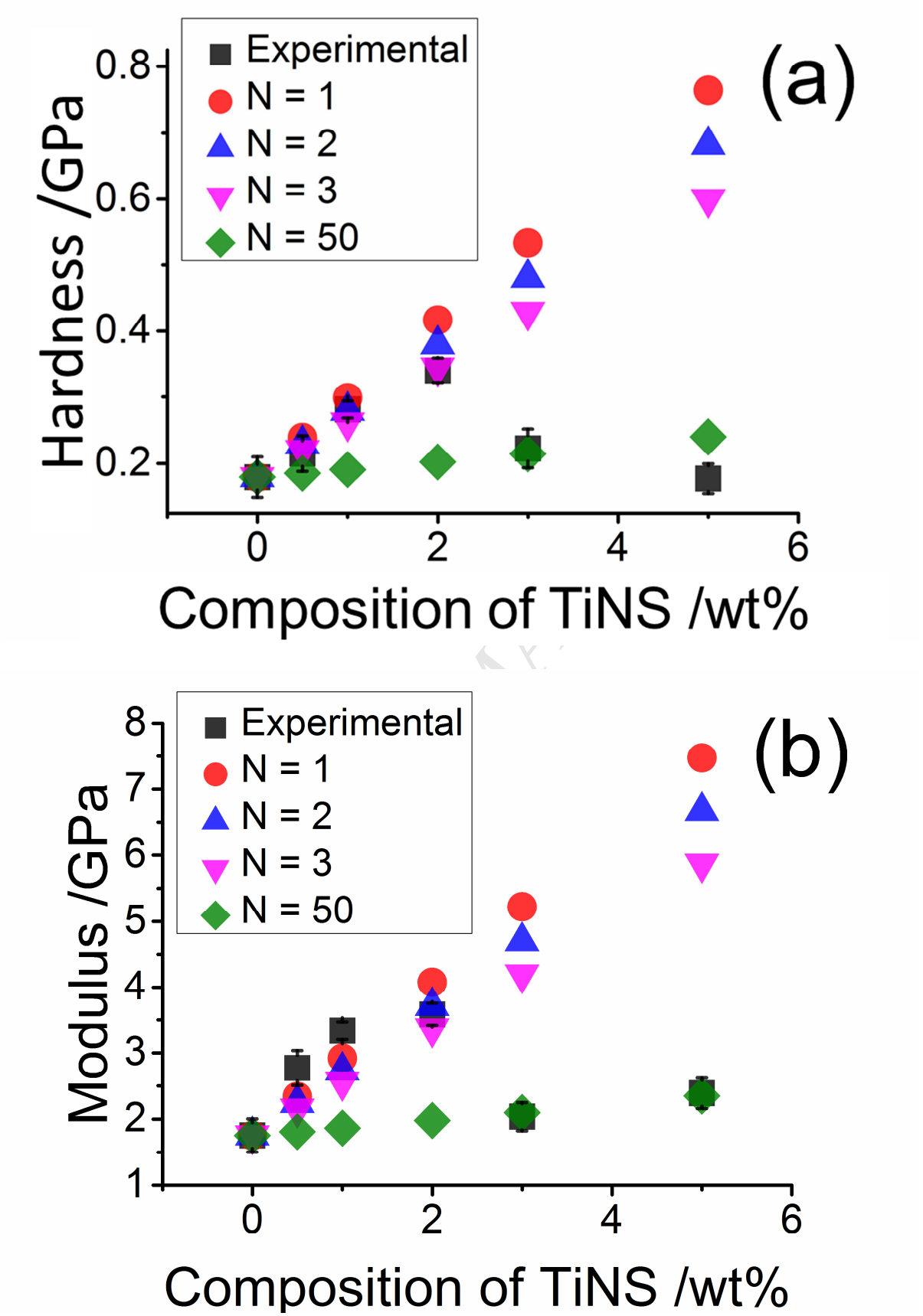
Experimental
N = 1
N = 2
N = 3
N = 50
(a)
Hardness /GPa
0.8
0.6
0.4
0.2
0
2
4
6
Composition of TiNS /wt%
Experimental
N = 1
N = 2
N = 3
N = 50
(b)
Modulus /GPa
8
7
6
5
4
3
2
1
0
2
4
6
Composition of TiNS /wt%

Figure 6

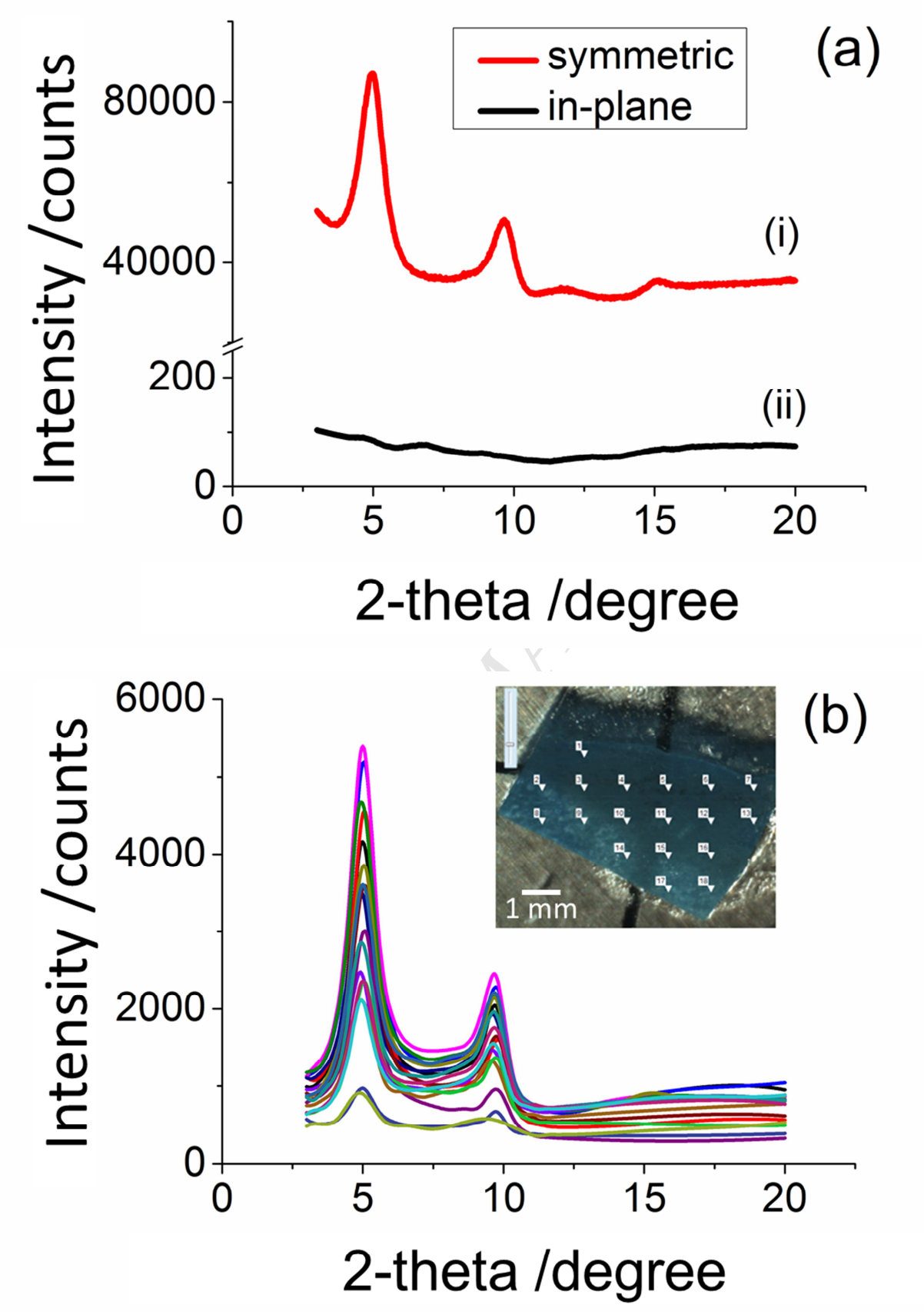
(a)
symmetric
in-plane
(i)
(ii)
Intensity /counts
80000
40000
200
0
0
5
10
15
20
2-theta /degree
(b)
1 mm
Intensity /counts
6000
4000
2000
0
0
5
10
15
20
2-theta /degree

Figure 7

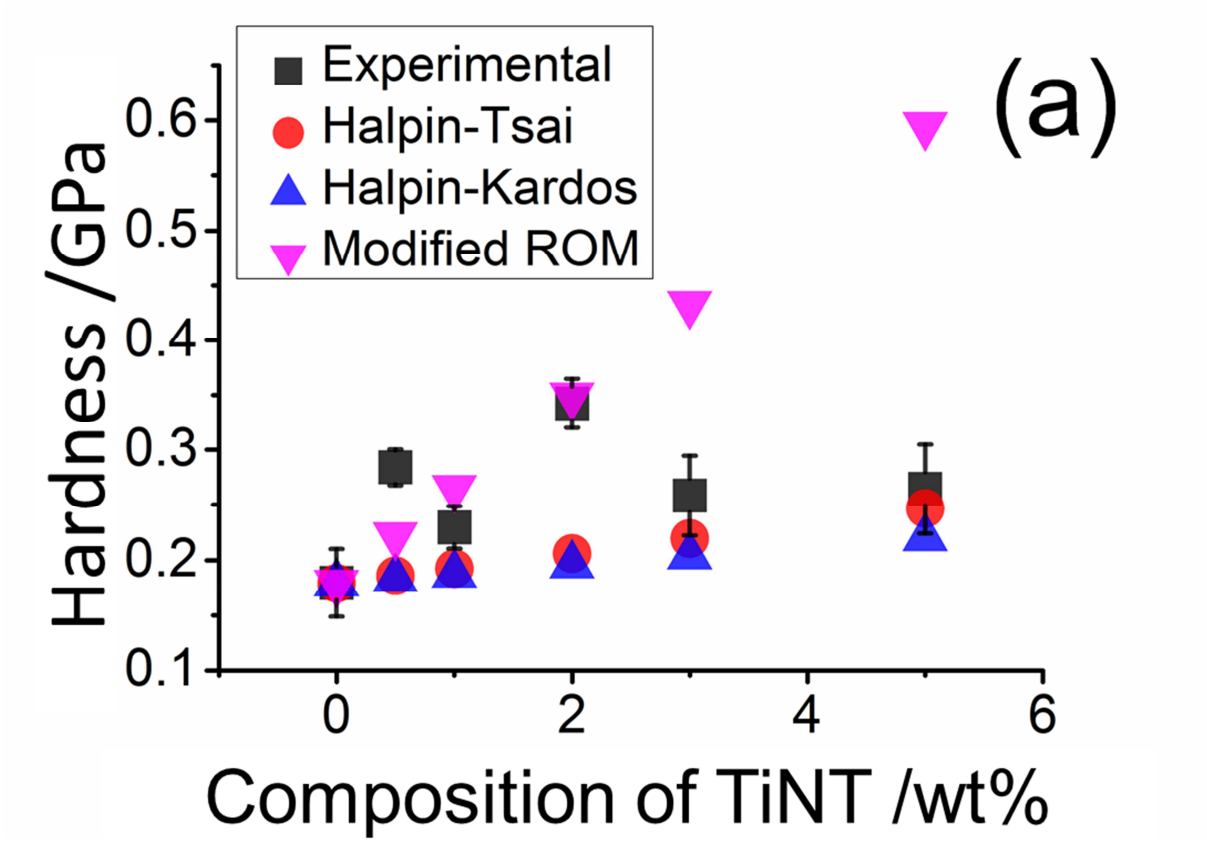
Experimental
Halpin-Tsai
Halpin-Kardos
Modified ROM
(a)
Hardness /GPa
0.1
0.2
0.3
0.4
0.5
0.6
0
2
4
6
Composition of TiNT /wt%

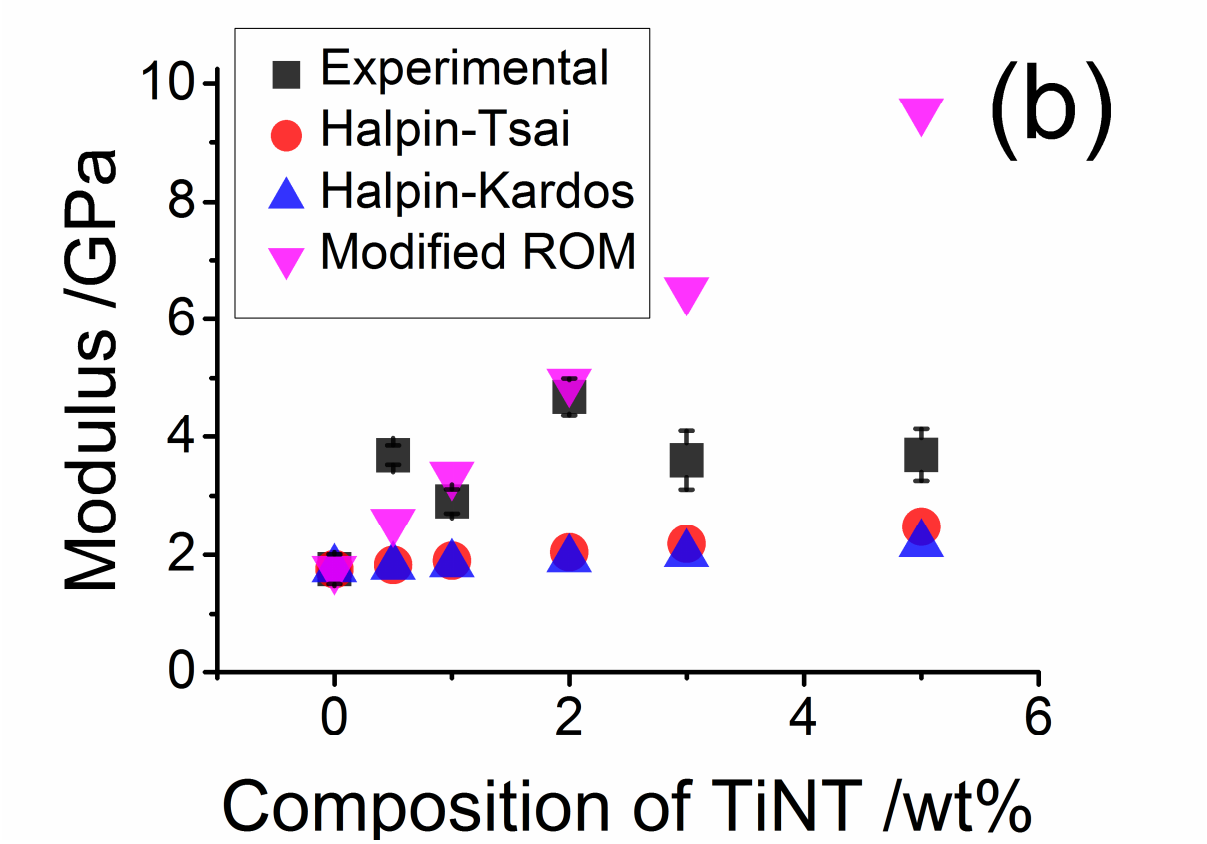
Experimental
Halpin-Tsai
Halpin-Kardos
Modified ROM
(b)
Modulus /GPa
0
2
4
6
8
10
0
2
4
6
Composition of TiNT /wt%

Figure 8

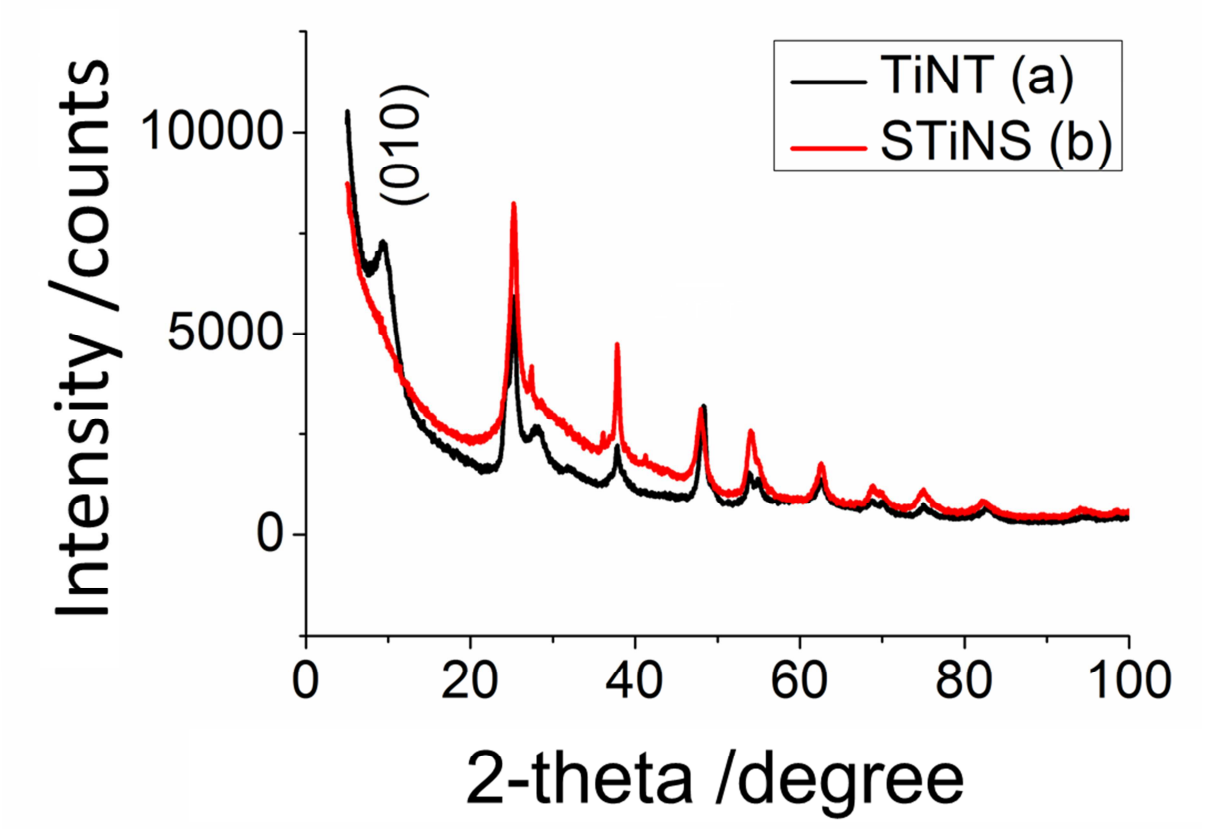

Figure 9

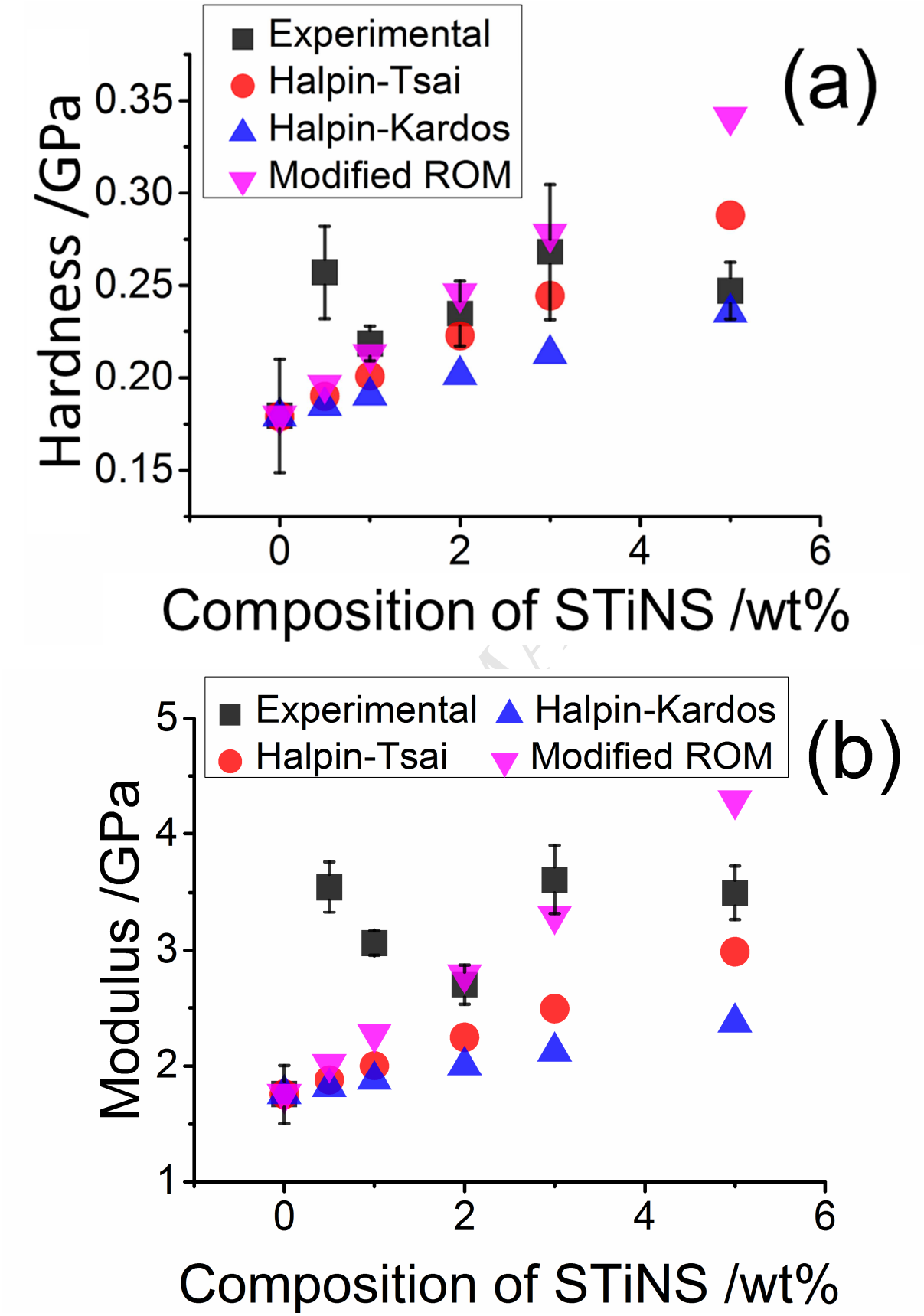
Experimental
Halpin-Tsai
Halpin-Kardos
Modified ROM
(a)
Hardness /GPa
0.35
0.30
0.25
0.20
0.15
0
2
4
6
Composition of STiNS /wt%
Experimental
Halpin-Kardos
Halpin-Tsai
Modified ROM
(b)
Modulus /GPa
5
4
3
2
1
0
2
4
6
Composition of STiNS /wt%

Figure 10

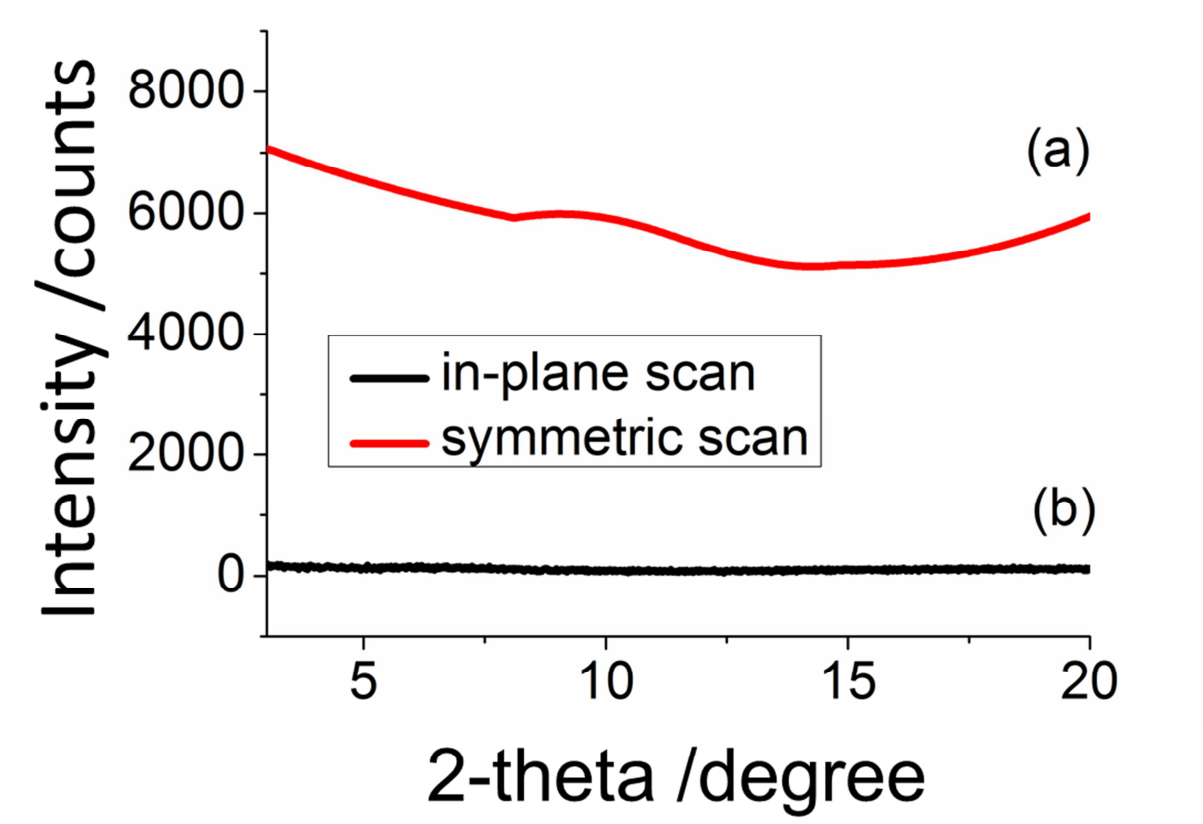

Figure S1 Combined SAXS & WAXS measurement for 5 wt% titanate nanotubes within polymer (a) symmetric scan (red); (b) in-plane scan (black). Neither shows any significant peaks due to alignment. In-plane scans are always of much lower intensity.

Highlights:

1. **Experimental and theoretical study** about reinforcement of nanocomposites mechanical properties **by titanate nanosheets, nanotubes, and scrolled nanosheets**
2. **Orientation of titanate** nanotubes and nanosheets within polymer matrix, intercalation of polymer inside nanosheets layer, and nanosheets exfoliation are **proven by Small-angle X-ray spectroscopy (SAXS)**
3. The Brune-Bicerano model, which is a **model for incomplete exfoliation of nanosheets**, has been used **to study agglomeration of nanosheets**